



## RESEARCH ARTICLE

WILEY polymers  
advanced  
technologies

# Preparation and evaluation of poly glycerol sebacate/poly hydroxy butyrate core-shell electrospun nanofibers with sequentially release of ciprofloxacin and simvastatin in wound dressings

Parisa Heydari<sup>1</sup> | Jaleh Varshosaz<sup>2</sup> | Anousheh Zargar Kharazi<sup>1</sup> | Saeed Karbasi<sup>1</sup>

<sup>1</sup>Biomaterials Nanotechnology and Tissue Engineering Faculty, School of Advanced Medical Technology, Isfahan University of Medical Sciences, Isfahan, Iran

<sup>2</sup>School of Pharmacy and Pharmaceutical Sciences, Isfahan University of Medical Sciences, Isfahan, Iran

**Correspondence**

Anousheh Zargar Kharazi, Biomaterials Nanotechnology and Tissue Engineering Faculty, School of Advanced Medical Technology, Isfahan University of Medical Sciences, Isfahan 8174673461, Iran.

Email: a\_zargar@med.mui.ac.ir;  
anosh\_zargar@yahoo.com

**Funding information**

Vice-Chancellery for Research and Technology of the Isfahan University of Medical Sciences

Biodegradable wound dressing of poly glycerol sebacate/poly hydroxy butyrate was fabricated via the coaxial electrospinning process. Simvastatin and ciprofloxacin were loaded in the core and shell of the fibers, respectively. Scanning electron microscopy and transmission electron microscopy images showed a uniform core/shell structure. Introducing drugs into the polymers would cause the dressing samples to become more hydrophilic and degradation to occur faster. Drugs release would face no interventions, in which, approximately 60% of ciprofloxacin was released during the first 24 hours. Simvastatin exhibited a slower and controlled release behavior, with its release peak recorded after 2 days. The drug-containing samples showed a proper bactericidal activity against both Gram-positive and Gram-negative bacteria. It may be concluded that the drug-laden wound dressing fabricated in this study is capable of releasing the 2 drugs sequentially and that it is the ideal conditions for controlling infections and reducing wound healing duration.

**KEYWORDS**

antibacterial, anti-inflammatory, coaxial electrospinning, drug delivery, PGS/PHB

## 1 | INTRODUCTION

Covering an area of about 2 m<sup>2</sup> and representing approximately one-tenth of the body mass, skin is the largest body organ.<sup>1</sup> It protects the body against a wide range of physical, mechanical, chemical, and pathogenic attacks. However, it is inevitably and frequently subjected to various injuries, such as burns, trauma, and chronic and diabetic ulcers.<sup>2,3</sup>

Partial-thickness wounds naturally heal without the need for any special treatment. However, burns and chronic diabetic ulcers as the most common causes of major losses (ie, full-thickness wounds) do not heal naturally but require external and long-standing treatments.<sup>4,5</sup> The conventional golden standard method so far is to treat those severe injuries by skin grafting. The limitations are not, however, only restricted to donor site shortage, scar formation, pain, tissue contracture, and other long-term complications.<sup>6</sup>

The healing process can be promoted by using biocompatible wound dressing materials. An ideal wound dressing should prevent dehydration of the wound and retain a favorable moist environment at the wound interface, allowing gas permeation as a barrier against dust and microorganisms. Furthermore, it should be nonadhesive, able to be easily removed without trauma, accelerate the wound healing

process, and deliver a nearly instantaneous initial dosage of drugs at optimum therapeutic concentrations.<sup>7,8</sup>

Natural materials extensively used to fabricate wound dressings include collagen,<sup>9</sup> chitosan,<sup>10</sup> silk fibroin,<sup>11</sup> alginate,<sup>12</sup> and hyaluronic acid.<sup>13</sup> In several studies, such synthetic polymers as polylactic acid,<sup>14</sup> polycaprolactone,<sup>15</sup> polyethylene glycol,<sup>16</sup> polyvinyl alcohol,<sup>17</sup> and poly hydroxyl butyrate (PHB)<sup>18</sup> have been used to fabricate wound dressings.

The high importance attached to developing means to improve the wound healing process and to prevent infections simultaneously encouraged Unnithan et al<sup>19</sup> to produce dextran/polyurethane as a ciprofloxacin (CIP) HCl antibiotic carrier and Sh. Tohidi et al<sup>20</sup> to fabricate poly (lactic-co-glycolic acid)/chitosan electrospun membranes containing amoxicillin-loaded halloysite nanoclay for wound healing. Xiaolan Zhang et al<sup>6</sup> used porous poly (glycerol sebacate) (PGS) elastomer scaffolds for skin tissue engineering and showed the excellent biocompatibility of the polymer for use in wound dressings.

The electrospinning technique used in wound dressing fabrication is associated with such varied advantages as high surface-to-volume ratio, tunable porosity, and ability to mimic the extracellular matrix of the tissue. These properties not only lead to a high potential for

absorbing wound exudates and keeping the moisture microenvironment of the wounds but also enhance cytocompatibility.<sup>21</sup>

Among the electrospinning techniques, the core-shell systems are considered to have a multifaceted nature. For one thing, the technique is capable of producing a continuous double layer of nanofibers by electrospinning 2 materials encapsulating different kinds of drugs through a facile 1-step procedure.<sup>22,23</sup> Creating structures with 2 distinct parts, an inner one called the “core” and an outer one called the “shell” that completely encloses the inner core,<sup>24</sup> the technique has provided on-demand biomaterial platforms for drug delivery and tissue engineering.<sup>25,26</sup> The porous structure thus produced creates a potentially useful morphology for both drug delivery and use as wound dressing.<sup>27</sup> In full thickness wounds, the blood supply faces obstructions due to the destruction of local vessels. This, therefore, postpones wound healing and drug delivery.<sup>8,28</sup> Furthermore, the polymers used in wound dressings should have the ability to load and release drugs in a controlled manner while they also have the same flexibility as the skin.<sup>29</sup>

In this study, the coaxial electrospinning technique was used to produce a PGS/PHB wound dressing with the capability of releasing simvastatin (SIM) and CIP drugs at the wound site.

Poly glycerol sebacate is a polyester prepared by poly condensation of glycerol and sebacic acid. It is a tough, biocompatible elastomer with a linear hydrolytic degradation that makes it suitable for drug release.<sup>30</sup> Moreover, PGS exhibits behaviors similar to elastin and collagen that make it appropriate for engineering soft tissues such as the skin.<sup>31</sup>

Poly hydroxy butyrate is a biocompatible thermoplastic polyester with a high crystallinity of 50% to 70%.<sup>32</sup> Electrospun PHB fiber meshes have shown some success in wound dressing applications due to their high hydrophobicity and mechanical strength.<sup>18</sup>

Recent studies have revealed that bacterial infection and chronic inflammation are important factors in delayed wound healing due to oxidative stress, proteolysis, and impeding angiogenesis.<sup>33</sup>

Local release of SIM plays a crucial role in the regulation of angiogenesis and the treatment of acute inflammation.<sup>34</sup> Jun Asai<sup>35</sup> studied the topical application of SIM to observe that it would accelerate diabetic wound healing as a result of enhanced angiogenesis and lymphangiogenesis.

Ciprofloxacin released in the wound serves as an antibacterial agent. It is claimed to be effective on a wide range of infections caused by a large spectrum of gram-positive and gram-negative bacteria in both humans and animals.<sup>29,36</sup>

The PGS/PHB wound dressings containing anti-inflammation and antibacterial drugs have been claimed to be effective in the treatment of deep wounds. Using a hydrophobic polymer in the shell section and a hydrophilic polymer (PGS) in the core part of the fibers impart proper mechanical properties to the wound dressing to help the local release of drugs in a controlled manner.

## 2 | EXPERIMENTAL

### 2.1 | Materials and synthesis of PGS

Chloroform, dimethyl formamide (DMF), and trifluoroacetic acid (TFA) were purchased from Merck (Germany). Poly hydroxyl butyrate and

phosphate buffered saline (D-PBS) were purchased from Sigma-Aldrich (USA). Ciprofloxacin and simvastatin powders were purchased from Alborz Pharmaceutical Company (Iran).

Briefly, the PGS prepolymer was synthesized via condensation polymerization as described in the literature.<sup>31,37</sup> Sebacic acid (purity 99%) and glycerol (purity 99%) were purchased from Merck (Germany). A mixture of sebacic acid and glycerol at a molar ratio of 1:1 was heated at 120°C for 24 hours under the N<sub>2</sub> atmosphere and the reactant was kept under vacuum at 40°C for 24 hours.<sup>30,38</sup> Finally, a white and viscous PGS prepolymer was obtained.

### 2.2 | Wound dressing preparation via coaxial electrospinning

Poly hydroxyl butyrate 7% w/v and CIP powder 10% v/v were dissolved in the trifluoroacetic acid solvent independently from each other before they were combined to make the shell solution. Similarly, PGS 30% w/v and SIM 5% v/v powder were dissolved in chloroform/dimethyl formamide (8:2 v/v) solvents to form the core part. Figure 1 presents a schematic diagram of the coaxial electrospinning process. Coaxial electrospinning needle consists of an inner tube 1.6 mm in diameter and an outer one 2 mm in diameter. A voltage ranging from 30 to 35 kV was applied at the tip of the spinneret. The feed flow rates to the core and the shell ranged from 0.1 to 1 mL/h, 0.2 to 1 mL/h, and 0.3 to 1 mL/h. The tip-to-collector distance was kept at 18 cm. All the electrospinning process was conducted at a temperature of around 25°C and at a humidity of less than 30%. All the electrospun wound dressings thus prepared were vacuumed and dried at room temperature before the remaining solvents were removed.

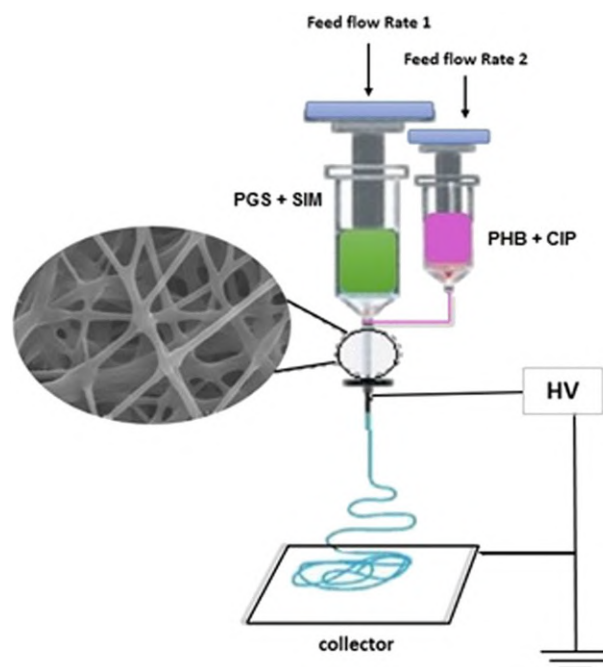


**FIGURE 1** Schematic of the coaxial electrospinning process. CIP, ciprofloxacin; PGS, poly glycerol sebacate; PHB, poly hydroxyl butyrate; SIM, simvastatin [Colour figure can be viewed at [wileyonlinelibrary.com](http://wileyonlinelibrary.com)]

## 2.3 | Characterization of drugs loaded PGS/PHB wound dressing

### 2.3.1 | Chemical characterization

Fourier-transform infrared spectroscopy (JASCO6300) in a range of 400 to 4000  $\text{cm}^{-1}$  was used to stabilize the chemical characteristics of the drug-containing and drug-free wound dressings also PGS prepolymer.

### 2.3.2 | Morphology of fibers

Scanning electron microscopy (SEM, SU3500, Hitachi, Japan) was used to evaluate the fiber diameter and porosity of the woven wound dressing structure. Prior to the process, the samples were coated with a thin layer of gold to produce a conductive surface. The surface of the samples was scanned at 15 kV. The mean pore diameter of the scaffolds was calculated using Image J software (National Institutes of Health, USA). The porosity of the wound dressing in SEM images was measured using the Matlab software (R 2012 a, The Mathworks Inc.) and expressed in percents.

### 2.3.3 | The core-shell structure

The core/shell structure of the coaxially electrospun fibers was studied using transmission electron microscopy (TEM, Zeiss-EM10C, Germany). Briefly, samples were prepared for TEM observation by putting carbon-coated copper grids on the collector where a very thin layer of electrospun fibers would be directly deposited. The copper grids containing nonstained fibers were then used to take TEM images by passing a beam of electrons through.<sup>23</sup>

### 2.3.4 | Contact angle measurement

The dynamic contact angle of the PGS/PHB wound dressing was measured using an optical contact angle measuring device. The tests were conducted under the contact angle drop model at a dosing volume of 4  $\mu\text{l}$ . The timer was started when the drop first touched the sample surface and separated from the needle. Pictures were captured by Charge Coupled Device (CCD) camera and the Image j software was used to determine contact angles. The reported values were mean  $\pm$  standard deviation ( $n = 3$ ).

### 2.3.5 | Water uptake ability (swelling)

To study the swelling kinetics, the membranes were cut into pieces 20  $\times$  5  $\text{mm}^2$  in size and the dry weights ( $W_d$ ) of the samples were recorded. The sample fibers were then immersed in the phosphate buffered saline (PBS) and their real-time wet weights ( $W_s$ ) were recorded. The degree of swelling was calculated using Equation 1 below:

$$\text{Degree of swelling\%} = [(W_s - W_d) / (W_d)] \times 100. \quad (1)$$

### 2.3.6 | Degradation studies

The degradation behavior of the samples was evaluated based on their mass loss. The specimens were cut to pieces 1  $\times$  1  $\text{mm}^2$  in size. The dry weights of the samples were then measured before being immersed in PBS at 37°C and monitored up to 3 weeks. At different time intervals (1, 4, 7, 14, and 21 days), the specimens were removed out of the PBS, rinsed with distilled water, and dried in a vacuum oven at room

temperature for 24 hours. Finally, the mass of each membrane was measured to determine degradation rate using Equation 2 below:

$$\text{Weight loss\%} = [(W_1 - W_2) / (W_1)] \times 100, \quad (2)$$

where  $W_1$  and  $W_2$  represent the initial weight of the sample and the real-time dry weight of the degraded samples, respectively ( $n = 3$ , for each group).

## 2.4 | Drug entrapment efficiency

Using ultraviolet-visible spectroscopy (UV-VIS, Shimadzu, Japan), the amounts of the drug samples (SIM/CIP) dissolved in PBS were measured and compared with those loaded during the electrospinning process. Drug entrapment efficiency of the wound dressings prepared with the polymers in fiber meshes was calculated using Equation 3 below:

$$\% \text{Entrapment efficiency} = (\text{Estimated percent drug content} / \text{theoretical percent drug content}) \times 100. \quad (3)$$

## 2.5 | In vitro drug release studies

To measure drug release from the electrospun PGS/PHB wound dressings containing SIM/CIP, a known area of (2.5  $\times$  2.5  $\text{cm}^2$ ) the sample was immersed in 10 mL of PBS ( $n = 3$ ). The samples soaked in PBS were then transferred into a shaker incubator where they were shaken at 37°C for 150 hours. At given intervals after immersion in PBS (namely, 15 minutes, 30 minutes, 1, 2, 4, 6, 12, 24, 48, 72, and 96 hours), a known volume of the solution was taken to determine the release kinetics of SIM and CIP using UV-VIS spectrophotometry. The absorbance peaks were recorded at 271 and 249 nm wavelengths for CIP and SIM, respectively.

## 2.6 | Antibacterial testing

The antibacterial activity of the drug-containing and drug-free PGS/PHB samples was evaluated using the disk diffusion method.<sup>19</sup> Both gram-negative *Escherichia coli* and gram-positive *Staphylococcus aureus* bacteria were used in the nutrient Hinton agar environment. Briefly, the specimens were cut into small circular disks of around 7 mm in diameter and placed on the surface of the Petri dishes. The antibacterial activity plates were incubated at 37°C, and the diameter of the inhibition zone on each plate was measured after 24 hours.

## 2.7 | Statistical analysis

Test results were presented as means  $\pm$  standard deviation. The one-way analysis of variance was used, and differences were declared statistically significant at  $P < .05$ .

# 3 | RESULTS AND DISCUSSION

## 3.1 | Chemical characterization of PGS and PGS/PHB wound dressings

The Fourier-transform infrared spectrum of the PGS obtained shows a broad absorption peak of hydroxyl groups at 3458  $\text{cm}^{-1}$  and sharp

peaks of methyl and alkane groups at 2925 and 2853  $\text{cm}^{-1}$  respectively. The peaks at 1731 and 1171  $\text{cm}^{-1}$  originating from C=O and C–O stretching vibrations confirm the formation of ester bonds and reveal the successful synthesis of PGS (Figure 2A).<sup>19,27</sup>

The chemical composition of PGS/PHB core-shell structure is presented in Figure 2B. The measurement peaks included 1044  $\text{cm}^{-1}$  (C–CH<sub>3</sub> stretching), 1054  $\text{cm}^{-1}$  (C–O), 1130  $\text{cm}^{-1}$  CH<sub>3</sub> rocking), 1224  $\text{cm}^{-1}$  (C–O–C stretching), 1287  $\text{cm}^{-1}$  (CH), 1380  $\text{cm}^{-1}$  (CH<sub>3</sub>), and 1450  $\text{cm}^{-1}$  (C=O stretching), all belonging to PHB.<sup>39</sup> It should be noted that all the PGS peaks shown in Figure 2A were also observed. This means that neither did any change occur in the chemical structure of the polymers nor were any new bands created in their structures.

The spectrum of SIM presented characteristic sharp peaks at 3550.31  $\text{cm}^{-1}$  (alcoholic O–H stretching vibration), 2875.34  $\text{cm}^{-1}$  (methyl and methylene C–H asymmetric and symmetric stretching vibration), and 1464.67 and 1388.50  $\text{cm}^{-1}$  (methyl and methylene C–H bending vibration).<sup>40</sup> In another site, bands at 1707, 1624, and 1268  $\text{cm}^{-1}$  were assigned for CIP to the C=O stretching vibration of the carboxyl group, the ketone C=O stretching vibration, and coupling of the carboxyl C–O stretching and O–H deformation vibrations, respectively.<sup>41</sup> Figure 2C shows the peaks of the 2 polymers and the 2 drugs in the wound dressing structure. It is seen that no change occurred in the chemical structure of the 2 polymers and that the drugs were located separately in the core and in the shell.

### 3.2 | Morphology of the PGS/PHB core/shell fibers

The morphologies of the coaxially electrospun PGS/PHB fibers with and without the drugs are shown in Figure 3A–E. The presence of drugs in the structure and the different core-to-shell flow rates of electrospinning are the 2 factors that bring about morphological changes in the fibers. The results of electrospinning PGS/PHB at a flow rate of 0.1:1 are provided in Figure 3A. Figure 3B shows the same fibers when the drugs were added, but no change was made in the feeding rate. Clearly, the structure was twisted, and the fibers were ill-formed. Figure 3C shows the morphologies of the samples fabricated at a flow rate of 0.2:1; adding drugs led to a smooth surface and a uniform structure while adding no drugs led to the formation of beads (Figure 3D).

Figure 3E, F presents the results for a flow rate of 0.3:1 with and without drugs, respectively. Clearly, these fibers were sticking and

exhibited undesirable conditions. Thus, a flow rate of 0.2:1 was chosen for the fabrication of fibers.

The challenge in electrospinning of PGS lies in the low viscosity of the polymer solution that makes it difficult to form continuous fibers.<sup>31</sup> In this study, it was observed that insertion of PHB in the shell made it easier to form continuous PGS fibers using the coaxial electrospinning method. The average diameter and porosity of the fibers thus formed were measured and reported in Table 1.

Based on the SEM images, the average diameter of PGS/PHB fibers fabricated at the ideal rate of 0.2:1 was about 745±70.2 nm and that of PGS/PHB fibers containing drugs (SIM/CIP) was about 575±40.6 nm. It is clear that fiber diameter depends directly on solution viscosity so that higher viscosities led to larger fiber diameters. Moreover, it is seen that viscosity declined when drugs were added to the polymer solution, which resulted in reduced fiber diameter.<sup>25</sup>

Porosity is also found to be an important parameter as it possibly causes gas permeation in the wound dressing and cell cultures.<sup>33</sup> The mean pore size of the samples was measured to be about 84%, and no significant differences were observed when the drugs were introduced into the structure.

### 3.3 | Core/shell structure of PGS/PHB fibers

As already seen, flow rate plays a major role in the electrospinning of polymer solutions.<sup>42</sup> Based on the above observations, the appropriate flow rate for the drug-containing PGS/PHB fibers is 0.2:1 mL/h. Figure 4 shows TEM images of the PGS/PHB with SIM/CIP core/shell structure. Clearly, separate shell and core were created in the structure with the core completely encapsulated in the shell so that the fibers thus formed were able to load 2 different drugs simultaneously.

### 3.4 | Contact angle of the samples

The contact angles of pure PHB, PGS/PHB, and drug-laden PGS/PHB core-shell electrospun samples were measured (Figure 5). Poly hydroxyl butyrate fibers exhibited a hydrophobic nature with a contact angle of 116.56 ± 5.1° (Figure 5A). Based on Figure 5B, the contact angle of PGS/PHB reached 53.2 ± 3.6° probably due to the increasing diameter of the fibers since the core-shell method increased surface roughness that, in turn, made the specimen more hydrophilic. When

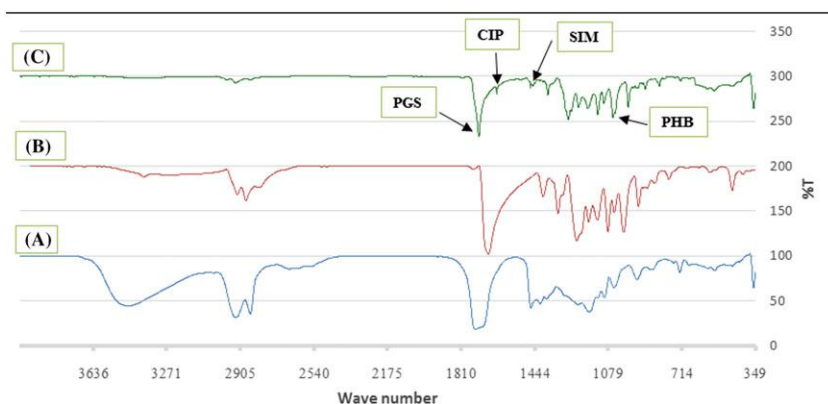


**FIGURE 2** Fourier-transform infrared spectra of A, poly glycerol sebacate (PGS), B, PGS/poly hydroxyl butyrate (PHB) fibers, (C) PGS/PHB fibers loaded with simvastatin (SIM)/ciprofloxacin (CIP) [Colour figure can be viewed at [wileyonlinelibrary.com](http://wileyonlinelibrary.com)]

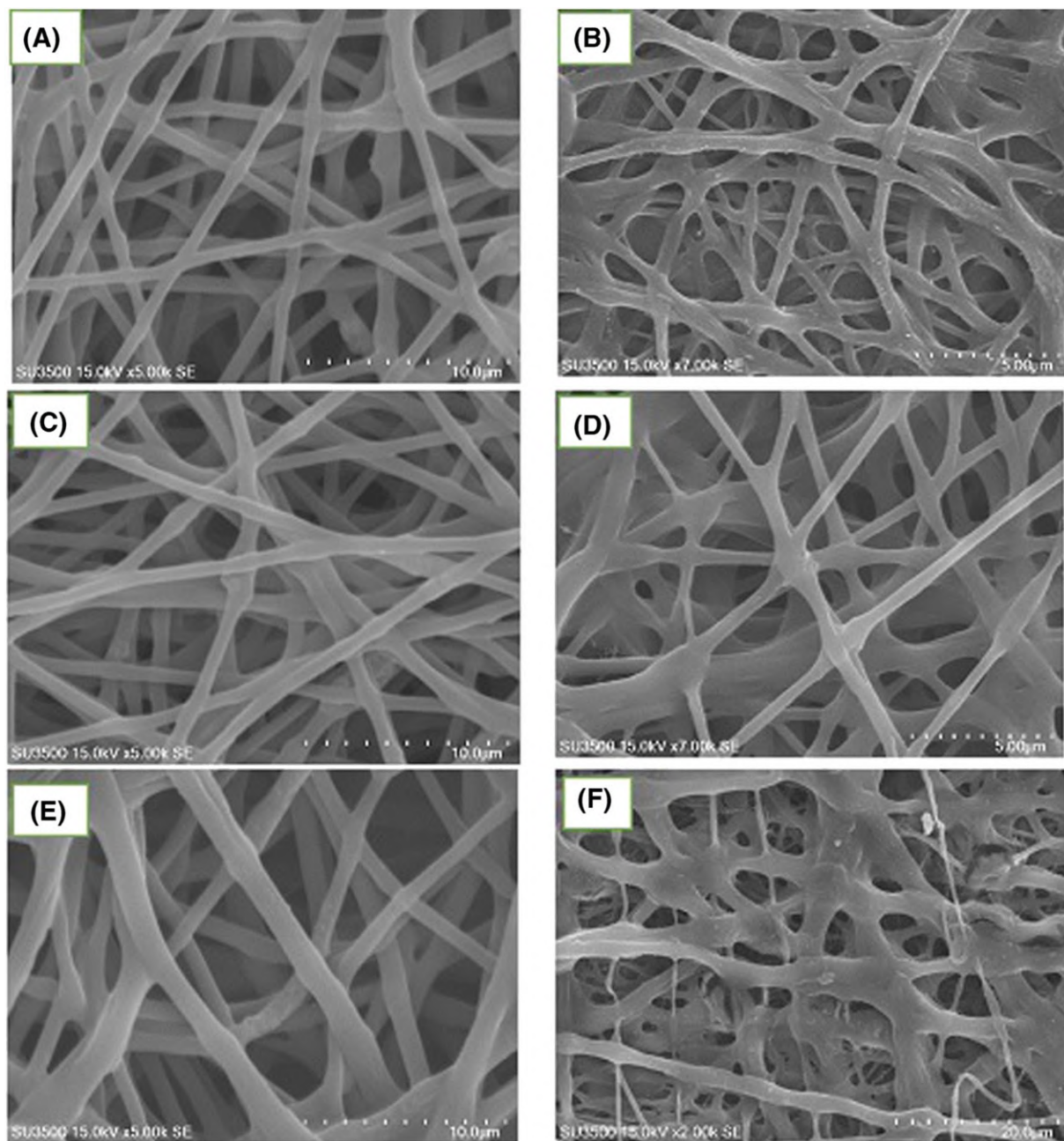


**FIGURE 3** Scanning electron microscopy images of electrospun fibers from PGS/PHB core-shell prepared at different inner solution flow rates and with or without drugs: A, 0.1 mL/h, B, 0.1 mL/h with drugs, C, 0.2 mL/h, D, 0.2 mL/h with drugs, E, 0.3 mL/h, F, 0.3 mL/h with drugs. PGS, poly glycerol sebacate; PHB, poly hydroxyl butyrate [Colour figure can be viewed at [wileyonlinelibrary.com](http://wileyonlinelibrary.com)]

**TABLE 1** Electrospun fiber diameter and porosity

	Sample Flow Rate, mL/h	Average Fibers Diameter, nm	Porosity, %
1	0.1:1	648 ± 58.5	84.7
2	0.2:1	745 ± 70.2	83.0
3	0.3:1	1161 ± 279.9	85.2
4	0.1:1 with ciprofloxacin and simvastatin	448 ± 88.5	86.1
5	0.2:1 with ciprofloxacin and simvastatin	575 ± 40.6	84.5
6	0.3:1 with ciprofloxacin and simvastatin	1427 ± 258.2	85.4

the drugs were added to these polymers, the contact angle declined to  $24.67 \pm 6.02^\circ$  due to the presence of the hydrophilic CIP drug in the shell of the fibers (Figure 5C).

By using the coaxial electrospinning method of PGS/PHB and the addition of drugs to this structure, the fibers got more hydrophilic, which is an ideal characteristic of a wound dressing.<sup>43</sup>

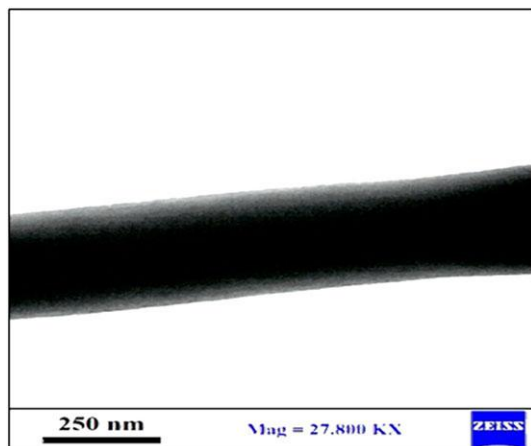


**FIGURE 4** Transmission electron microscopy images of the coaxially electrospun composite fibers of the PGS/PHB loaded with SIM/CIP. CIP, ciprofloxacin; PGS, poly glycerol sebacate; PHB, poly hydroxyl butyrate; SIM, simvastatin [Colour figure can be viewed at wileyonlinelibrary.com]

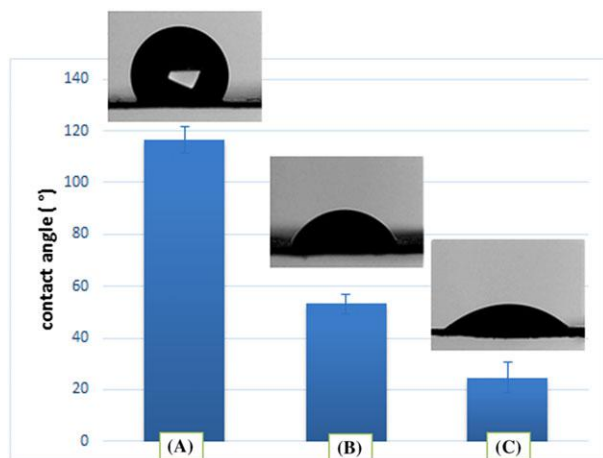


**FIGURE 5** Water contact angles for A, PHB, B, PGS/PHB, and C, PGS/PHB-SIM/CIP. CIP, ciprofloxacin; PGS, poly glycerol sebacate; PHB, poly hydroxyl butyrate; SIM, simvastatin [Colour figure can be viewed at wileyonlinelibrary.com]

### 3.5 | Water uptake ability (swelling) of the fibers

The degree of swelling of a wound dressing plays an important role not only in the loading and release behavior of drugs but also in the amount of wound exudates absorbed. According to Figure 6A, Equation 1 yielded swelling degrees of  $83.09 \pm 4.9\%$ ,  $104.45 \pm 6.3\%$ ,  $115.25 \pm 9.91\%$ , and  $122.53 \pm 12.45\%$  for the PGS/PHB electrospun samples for time intervals of 18, 24, 36, and 60 hours, respectively. Poly glycerol sebacate is a hydrophilic polymer forming the inner core of the sample while PHB is a hydrophobic one forming the outer shell of the fibers. The electrospun PGS/PHB wound dressing has a porous structure with a high specific surface area into which liquids can penetrate to cause it to swell. An ideal dressing is normally characterized by a water absorption rate of 100% to 900%, a high wettability, and a contact angle lower than  $90^\circ$ .<sup>43</sup> Wang et al<sup>44</sup> showed that the high absorption of collagen/hyaluronic acid/gelatin samples was suitable for skin regeneration.

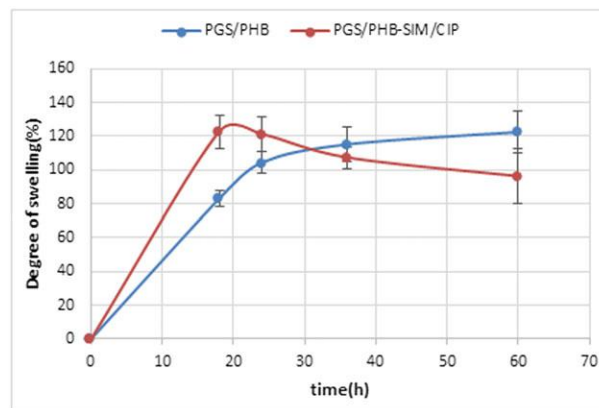


**FIGURE 6** Swelling degree in PBS for PGS/PHB and PGS/PHB-SIM/CIP. CIP, ciprofloxacin; PGS, poly glycerol sebacate; PHB, poly hydroxyl butyrate; SIM, simvastatin [Colour figure can be viewed at wileyonlinelibrary.com]

In the electrospun PGS/PHB sample containing SIM and CIP, the swelling degrees in the PBS were obtained to be  $122 \pm 9.96\%$ ,  $121.32 \pm 10.49$ ,  $107.45 \pm 6.45\%$ , and  $96.39 \pm 16.02\%$  for the above time intervals (Figure 6B). In the drug-containing samples, the degradation onset combined with the drug release had an escalating effect on weight loss after the first 18 hours.

### 3.6 | Wound dressing degradation test

Degradation behavior was also evaluated for PGS/PHB samples with and without drugs. The results showed that degradation takes a faster rate in samples containing drugs than in those without drugs (Figure 7). The presence of drugs in the structure and their release in the PBS facilitated water penetration into the structure, which resulted in accelerated degradation. At the end of the first 21 days, the drug-containing PGS/PHB and those lacking drugs lost around 45% and 28% of their weights, respectively. The samples disintegrated after 21 days, and the degradation test was consequently terminated.

Moreover, severe weight losses were observed due to the synergic effect of drug release and polymer chain degradation during the first 4 days. From day 5 onwards, however, only the polymers underwent degradation so that a decline was observed in the degradation rate.

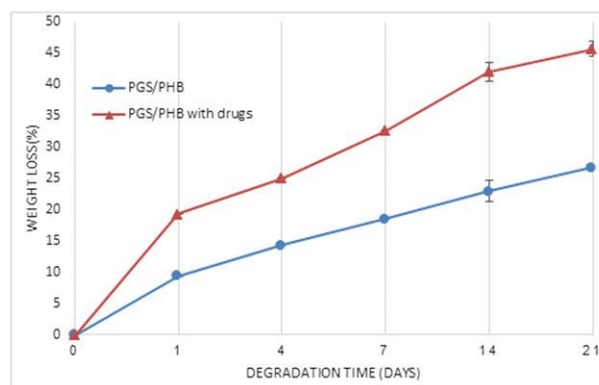


**FIGURE 7** Degradation curves following soaking in PBS for PGS/PHB and PGS/PHB with drugs. PGS, poly glycerol sebacate; PHB, poly hydroxyl butyrate [Colour figure can be viewed at wileyonlinelibrary.com]

### 3.7 | Drug entrapment efficiency of wound dressing

Drugs loading of the core-shell electrospun samples led to CIP and SIM entrapment efficiencies of 96% and 85%, respectively. Normally, electrospinning allows the polymer solution to contain maximum drug loading. The difficulties faced with in electrospinning PGS, however, lead to a reduced SIM entrapment efficiency. For this reason, release kinetics studies were simultaneously conducted for both drugs.

### 3.8 | In vitro drug release studies

The rates of CIP and SIM release from electrospun samples (PGS/PHB) in PBS are presented in Figure 8. The release of hydrophilic drugs from the samples takes place in 3 steps: water diffusion into

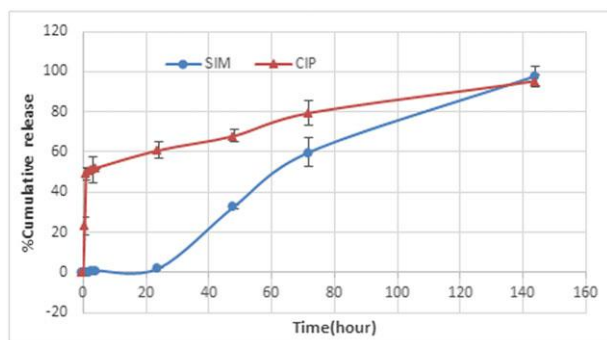


**FIGURE 8** Ciprofloxacin and simvastatin release profiles from the electrospun poly glycerol sebacate/poly hydroxyl butyrate fibers in PBS at 37°C. CIP, ciprofloxacin; SIM, simvastatin [Colour figure can be viewed at [wileyonlinelibrary.com](#)]

the fiber, drug dissolution, and drug diffusion out of the sample into PBS.<sup>45</sup> In the PGS/PHB core-shell fibers, the PBS initially enters the fiber shell and dissolves CIP before the release period starts. It can be seen that the CIP in the wound dressing was associated with a fast release (ie, ~60% in 24 hours). This abrupt release is due to the hydrophilic nature of CIP which causes it to be stored in the shell of the fibers.

In the case of SIM, the release of the drug begins after 24 hours at a low delivery rate. The reason for the slow and controlled release of SIM is its storage in the core portion of the fibers and the sheathing of the hydrophobic PHB polymer. In addition, SIM is a hydrophobic drug, which causes it to enter the PBS only after the onset of the polymeric chain degradation. Based on the results of the degradation test, it may be claimed that the slow release of this drug is due to the linear degradation behavior of PGS.<sup>30</sup>

The differences between the release and delivery rates of CIP and SIM offer the potential for achieving improved wound healing, reduced inflammation, and prevention of infections at the wound site. These advantages make this sample an ideal wound dressing.

### 3.9 | Antibacterial test

Antibacterial test results can be beneficially exploited in fabricating wound dressings as wounds often get infected with bacterial species, especially during the first 24 hours, which inevitably adds to complications and makes the treatment procedures more complex, thus slowing down the healing process. It would be, therefore, desirable to fabricate wound dressings with antibacterial properties.<sup>18</sup> Figure 9 shows the antibacterial test results for the PGS/PHB wound dressing, indicating

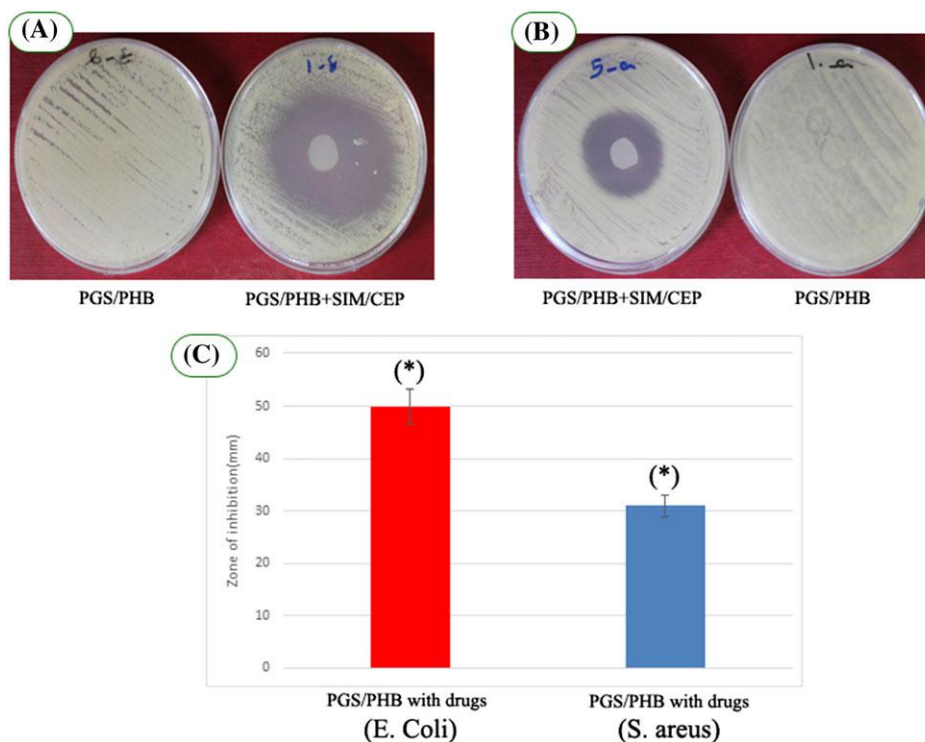


**FIGURE 9** Antibacterial activity of PGS/PHB fibers loaded with SIM/CIP against A, *E. coli*, B, *S. aureus*, and C, sizing of the inhibition zone. The (\*) shows statistically significant differences in  $n = 3$  ( $P < .05$ ). CIP, ciprofloxacin; *E. coli*, *Escherichia coli*; PGS, poly glycerol sebacate; PHB, poly hydroxyl butyrate; SIM, simvastatin; *S. aureus*, *Staphylococcus aureus* [Colour figure can be viewed at [wileyonlinelibrary.com](#)]

significant differences between the 2 drug-containing and drug-free samples with respect to their inhibition zones against *E. coli* (Figure 9 A). Figure 9B shows the significantly large inhibition zone against *S. aureus* in samples containing drugs. Clearly, drug-containing wound dressings exhibited significantly large inhibition zones as compared to the drug-free PGS/PHB control fibers.

Figure 9C presents the sizes of the inhibition zones against different bacteria in these wound dressings. Drug loading was clearly effective against gram-negative (*E. coli*) and gram-positive (*S. aureus*) bacteria with inhibition zones of  $49.93 \pm 3.34$  mm and  $30.95 \pm 2$  mm, respectively, indicating the efficacy of the wound dressings in preventing infections with both types of bacteria.

In fact, it may be concluded that CIP is a drug that showed excellent bactericidal activity against the wide range of bacteria, therefore avoiding exogenous infections effectively.<sup>19</sup> The results showed that our sample is a proper antibacterial wound dressing and it can be applied as a perfect wound dressing material.

## 4 | CONCLUSIONS

In the present study, a novel biodegradable PGS/PHB wound dressing containing SIM/CIP was successfully fabricated by coaxial electrospinning. The physicochemical properties of the PGS/PHB samples with and without drugs were evaluated. The results showed that better core-shell fibers could be fabricated via the electrospinning process at a flow rate of 0.2:1 mL/h for both PGS and PHB. Introducing the SIM/CIP drugs into the structure was observed to reduce fiber diameters and make the wound dressing to become more hydrophilic.

Ciprofloxacin loaded in the shell part (PHB) of the fiber exhibited a bursting abrupt release, which facilitated the control of wound infections during the first 24 hours. Simvastatin, loaded in the core part of the fibers (PGS), however, exhibited a slow release rate, which allowed enough time for the wounds to heal. Investigation of the degradation process revealed that the release of SIM is affected by the linear degradation of PGS. The controlled release of CIP and SIM showed that the proposed wound dressing was not only able to contribute to the better prevention of infections but also to reduce inflammation at the wound site. Finally, the high antibacterial activity (large inhibition zones) against both gram-positive and gram-negative bacteria in the PGS/PHB laden with SIM/CIP, as compared with the PGS/PHB samples, confirm the capability of these samples for application in wound healing treatment.

## ACKNOWLEDGEMENT

The authors acknowledge the financial support from Vice-Chancellery for Research and Technology of the Isfahan University of Medical Sciences.

## ORCID

Parisa Heydari  <http://orcid.org/0000-0002-3907-5451>

Anousheh Zargar Kharazi  <http://orcid.org/0000-0001-8945-0144>

## REFERENCES

- Zhao X, Wu H, Guo B, Dong R, Qiu Y, Ma PX. Antibacterial anti-oxidant electroactive injectable hydrogel as self-healing wound dressing with hemostasis and adhesiveness for cutaneous wound healing. *Biomaterials*. 2017;122:34-47.
- Groeber F, Holeiter M, Hampel M, Hinderer S, Schenke-Layland K. Skin tissue engineering—in vivo and in vitro applications. *Adv Drug Deliv Rev*. 2011;63(4):352-366.
- Rieger KA, Birch NP, Schiffman JD. Designing electrospun nanofiber mats to promote wound healing—a review. *J Mater Chem B*. 2013;1(36):4531-4541.
- Morgado PI, Aguiar-Ricardo A, Correia IJ. Asymmetric membranes as ideal wound dressings: an overview on production methods, structure, properties and performance relationship. *J Memb Sci*. 2015;490:139-151.
- Shin YC, Shin D, Lee EJ, et al. Hyaluronic acid/PLGA core/shell fiber matrices loaded with EGCG beneficial to diabetic wound healing. *Adv Healthc Mater*. 2016;5(23):3035-3045.
- Zhang X, Jia C, Qiao X, Liu T, Sun K. Porous poly (glycerol sebacate) (PGS) elastomer scaffolds for skin tissue engineering. *Polym Test*. 2016;54:118-125.
- Ju HW, Lee OJ, Lee JM, et al. Wound healing effect of electrospun silk fibroin nanomatrix in burn-model. *Int J Biol Macromol*. 2016;85:29-39.
- Andreu V, Mendoza G, Arruebo M, Irusta S. Smart dressings based on nanostructured fibers containing natural origin antimicrobial, anti-inflammatory, and regenerative compounds. *Materials (Basel)*. 2015;8(8):5154-5193.
- Rastogi S, Modi M, Sathian B. The efficacy of collagen membrane as a biodegradable wound dressing material for surgical defects of oral mucosa: a prospective study. *J Oral Maxillofac Surg*. 2009;67(8):1600-1606.
- Aoyagi S, Onishi H, Machida Y. Novel chitosan wound dressing loaded with minocycline for the treatment of severe burn wounds. *Int J Pharm*. 2007;330(1):138-145.
- Bhardwaj N, Sow WT, Devi D, Ng KW, Mandal BB, Cho N-J. Correction: silk fibroin-keratin based 3D scaffolds as a dermal substitute for skin tissue engineering. *Integr Biol*. 2015;7(1):142.
- Venkatesan J, Jayakumar R, Anil S, Chalisserry EP, Pallela R, Kim S-K. Development of alginate-chitosan-collagen based hydrogels for tissue engineering. *J Biomater Tissue Eng*. 2015;5(6):458-464.
- Kim G, Ahn S, Kim Y, Cho Y, Chun W. Coaxial structured collagen-alginate scaffolds: fabrication, physical properties, and biomedical application for skin tissue regeneration. *J Mater Chem*. 2011;21(17):6165-6172.
- Garric X, Guillaume O, Dabboue H, Vert M, Molès J-P. Potential of a PLA-PEO-PLA-based scaffold for skin tissue engineering: in vitro evaluation. *J Biomater Sci Polym Ed*. 2012;23(13):1687-1700.
- Jin G, Prabhakaran MP, Kai D, Annamalai SK, Arunachalam KD, Ramakrishna S. Tissue engineered plant extracts as nanofibrous wound dressing. *Biomaterials*. 2013;34(3):724-734.
- Costache MC, Qu H, Ducheyne P, Devore DI. Polymer-xerogel composites for controlled release wound dressings. *Biomaterials*. 2010;31(24):6336-6343.
- Kang YO, Yoon I, Lee SY, et al. Chitosan-coated poly (vinyl alcohol) nanofibers for wound dressings. *J Biomed Mater Res Part B Appl Biomater*. 2010;92(2):568-576.
- Bhattacharjee A, Kumar K, Arora A, Katti DS. Fabrication and characterization of Pluronic modified poly(hydroxybutyrate) fibers for potential wound dressing applications. *Mater Sci Eng C*. 2016;63:266-273.
- Unnithan AR, Barakat NAM, Pichiah PBT, et al. Wound-dressing materials with antibacterial activity from electrospun polyurethane-dextran nanofiber mats containing ciprofloxacin HCl. *Carbohydr Polym*. 2012;90(4):1786-1793.
- Khalil KA, Fouad H, Elsarnagawy T, Almajhdi FN. Preparation and characterization of electrospun PLGA/silver composite nanofibers for biomedical applications. *Int J Electrochem Sci*. 2013;8:3483-3493.



21. Tohidi S, Ghaee A, Barzin J. Preparation and characterization of poly (lactic-co-glycolic acid)/chitosan electrospun membrane containing amoxicillin-loaded halloysite nanoclay. *Polym Adv Technol*. 2016;27(8):1020-1028.
22. Sedghi R, Shaabani A. Electrospun biocompatible core/shell polymer-free core structure nanofibers with superior antimicrobial potency against multi drug resistance organisms. *Polymer (Guildf)*. 2016;101:151-157.
23. Nguyen TTT, Chung OH, Park JS. Coaxial electrospun poly (lactic acid)/chitosan (core/shell) composite nanofibers and their antibacterial activity. *Carbohydr Polym*. 2011;86(4):1799-1806.
24. Gopinathan J, Indumathi B, Thomas S, Bhattacharyya A. Morphology and hydroscopic properties of acrylic/thermoplastic polyurethane core-shell electrospun micro/nano fibrous mats with tunable porosity. *RSC Adv*. 2016;6(59):54286-54292.
25. Sill TJ, von Recum HA. Electrospinning: applications in drug delivery and tissue engineering. *Biomaterials*. 2008;29(13):1989-2006.
26. Xu B, Rollo B, Stamp LA, et al. Non-linear elasticity of core/shell spun PGS/PLLA fibres and their effect on cell proliferation. *Biomaterials*. 2013;34(27):6306-6317.
27. Kharaziha M, Nikkha M, Shin S-R, et al. PGS: gelatin nanofibrous scaffolds with tunable mechanical and structural properties for engineering cardiac tissues. *Biomaterials*. 2013;34(27):6355-6366.
28. Cheng M-L, Lin Y-R, Lin Z-Z, Liao C-S, Sun Y-M. Physical and transport properties of polyhydroxybutyrate/clay nanocomposite membranes. *Tc*. 2014;87(96):87.
29. Ma X, Xiao Y, Xu H, Lei K, Lang M. Preparation, degradation and in vitro release of ciprofloxacin-eluting ureteral stents for potential antibacterial application. *Mater Sci Eng C*. 2016;66:92-99.
30. Rai R, Tallawi M, Grigore A, Boccaccini AR. Synthesis, properties and biomedical applications of poly (glycerol sebacate)(PGS): a review. *Prog Polym Sci*. 2012;37(8):1051-1078.
31. Xu B, Li Y, Zhu C, Cook WD, Forsythe J, Chen Q. Fabrication, mechanical properties and cytocompatibility of elastomeric nanofibrous mats of poly (glycerol sebacate). *Eur Polym J*. 2015;64:79-92.
32. Pachekoski WM, Agnelli JAM, Belem LP. Thermal, mechanical and morphological properties of poly (hydroxybutyrate) and polypropylene blends after processing. *Mater Res*. 2009;12(2):159-164.
33. Shevchenko RV, James SL, James SE. A review of tissue-engineered skin bioconstructs available for skin reconstruction. *J. R. Soc. Interface*, p. rsif20090403. 2009.
34. Farsaei S, Khalili H, Farboud ES. Potential role of statins on wound healing: review of the literature. *Int Wound J*. 2012;9(3):238-247.
35. Asai J, Takenaka H, Hirakawa S, et al. Topical simvastatin accelerates wound healing in diabetes by enhancing angiogenesis and lymphangiogenesis. *Am J Pathol*. 2012;181(6):2217-2224.
36. Liu L, Guo K, Lu J, et al. Biologically active core/shell nanoparticles self-assembled from cholesterol-terminated PEG-TAT for drug delivery across the blood-brain barrier. *Biomaterials*. 2008;29(10):1509-1517.
37. Li X, Hong AT-L, Naskar N, Chung H-J. Criteria for quick and consistent synthesis of poly (glycerol sebacate) for tailored mechanical properties. *Biomacromolecules*. 2015;16(5):1525-1533.
38. Kenar H, Kose GT, Toner M, Kaplan DL, Hasirci V. A 3D aligned microfibrillar myocardial tissue construct cultured under transient perfusion. *Biomaterials*. 2011;32(23):5320-5329.
39. Furukawa T, Sato H, Murakami R, et al. Structure, dispersibility, and crystallinity of poly (hydroxybutyrate)/poly (L-lactic acid) blends studied by FT-IR microspectroscopy and differential scanning calorimetry. *Macromolecules*. 2005;38(15):6445-6454.
40. Mandal D, Ojha PK, Nandy BC, Ghosh LK. Effect of carriers on solid dispersions of simvastatin (Sim): physico-chemical characterizations and dissolution studies. *Der Pharm Lett*. 2010;2(4):47-56.
41. Wu Q, Li Z, Hong H, Yin K, Tie L. Adsorption and intercalation of ciprofloxacin on montmorillonite. *Appl Clay Sci*. 2010;50(2):204-211.
42. Duan N, Geng X, Ye L, et al. A vascular tissue engineering scaffold with core-shell structured nano-fibers formed by coaxial electrospinning and its biocompatibility evaluation. *Biomed. Mater*. 2016;11(3, p. 35007).
43. Yuan Y, Lee TR. Contact angle and wetting properties. In: *Surface science techniques*. Berlin Heidelberg: Springer; 2013:3-34.
44. Wang H-M, Chou Y-T, Wen Z-H, Wang Z-R, Chen C-H, Ho M-L. Novel biodegradable porous scaffold applied to skin regeneration. *PLoS One*. 2013;8(6):e56330.
45. Yu H, Jia Y, Yao C, Lu Y. PCL/PEG core/sheath fibers with controlled drug release rate fabricated on the basis of a novel combined technique. *Int J Pharm*. 2014;469(1):17-22.

**How to cite this article:** Heydari P, Varshosaz J, Zargar Kharazi A, Karbasi S. Preparation and evaluation of poly glycerol sebacate/poly hydroxy butyrate core-shell electrospun nanofibers with sequentially release of ciprofloxacin and simvastatin in wound dressings. *Polym Adv Technol*. 2018;1-9. <https://doi.org/10.1002/pat.4286>